The American Journal of Human Genetics, Volume *93*

Supplemental Data

Defects in the IFT-B Component IFT172 Cause

Jeune and Mainzer-Saldino Syndromes in Humans

Jan Halbritter, Albane A. Bizet, Miriam Schmidts, Jonathan D. Porath, Daniela A. Braun, Heon Yung Gee, Aideen M. McInerney-Leo, Pauline Krug, Emilie Filhol, Erica E. Davis, Rannar Airik, Peter G. Czarnecki, Anna M. Lehman, Peter Trnka, Patrick Nitschké, Christine Bole-Feysot, Markus Schueler, Bertrand Knebelmann, Stéphane Burtey, Attila J. Szabó, Kálmán Tory, Paul J. Leo, Brooke Gardiner, Fiona A. McKenzie, Andreas Zankl, Matthew A. Brown, Jane L. Hartley, Eamonn R. Maher, Chunmei Li, Michel R. Leroux, Peter J. Scambler, Shing H. Zhan, Steven J. Jones, Hülya Kayserili, Beyhan Tuysuz, Khemchand N. Moorani, Alexandru Constantinescu, Ian D. Krantz, Bernard S. Kaplan, Jagesh V. Shah, UK10K Consortium, Toby W. Hurd, Dan Doherty, Nicholas Katsanis, Emma L. Duncan, Edgar A. Otto, Philip L. Beales, Hannah M. Mitchison, Sophie Saunier, and Friedhelm Hildebrandt

Supplemental Acknowledgments

This study used data generated by the UK10K Consortium. A full list of investigators who contributed to generate this data is available at www.uk10k.org. Part of this work was funded by FORGE Canada Consortium: Finding of Rare Disease Genes in Canada (leader Kym Boycott, University of Ottawa), with sequencing services provided by Canada's Michael Smith Genome Sciences Centre, Vancouver, Canada.

This research was further supported by grants from the National Institutes of Health to Friedhelm Hildebrandt (DK068306 and D K090917), to Edgar A. Otto (DK090917), to Dan Doherty (R01NS064077), to Nicholas Katsanis (DK072301 and HD042601), and to Erica E. Davis (EY021872); from the “Agence Nationale de la Recherche” (ANR) (R09087KS and RPV11012KK), the “Fondation pour la Recherche Médicale” (DEQ20071210558) to Sophie Saunier, and an Action Medical Research UK Clinical Training Fellowship towards Miriam Schmidts (RTF-1411).

Friedhelm Hildebrandt is an Investigator of the Howard Hughes Medical Institute, a Doris Duke Distinguished Clinical Scientist, and a Warren E. Grupe Professor of Pediatrics. H.M.M. is funded by the Newlife Foundation for Disabled Children UK and Action Medical Research UK (GN1773, GN2101). Philip L. Beales is a Wellcome Trust Senior Research Fellow and receives funding from the European Community’s Seventh Framework Program FP7/2009, under grant agreement no. 241955 SYSCILIA and Philip L. Beales and Miriam Schmidts received funds from the Dutch Kidney Foundation (CP11.18). The UK10K project is funded by the Wellcome Trust (Award WT091310). Sophie Saunier is an Investigator of the “Institut National de la Santé et de la Recherche Médicale” (INSERM) and Imagine Institute. Aideen M. McInerney-Leo is supported by a University of Queensland postgraduate student fellowship. Andreas Zankl is funded by the Royal Children’s Hospital Foundation and A NZ Trustee’s Children’s Medical Research Establishment Grant. Matthew A. Brown is supported by a National Health and Medical Research Council Senior Principal Research Fellowship. Nicholas Katsanis is a distinguished Jean and George Brumley Professor. Attila Fintha (2nd Dep. of Pathology, Semmelweis University Budapest, Hungary) and G ábor Rudas (Semmelweis University Budapest, MR Research Center, Hungary) contributed to the generation of data, used in this study. We also acknowledge funding from CIHR (grant MOP-82870) to Michel R. Leroux.

The help of Ms. Mhairi Marshall, Ms. Jessica Harris, Ms. Sharon Song, Ms. Lisa Anderson, Mr. Atif Alsaedi, Mr. Jason Willer and discussion with Dr. Carol Wicking is gratefully acknowledged.

NPH2218

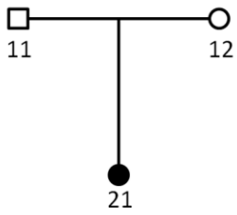

c.432delA
p.[Lys144Asnfs*76];[=]

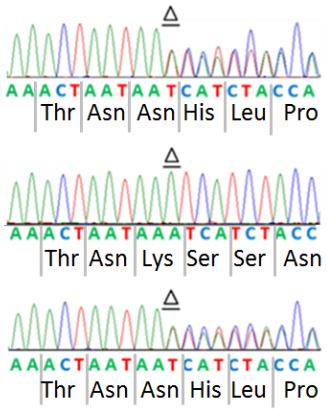

a

c.4161G>A
p.[Arg1387Serfs*7];[=]

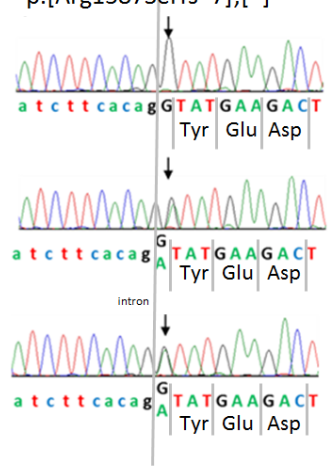

A3189

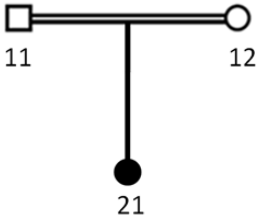

c.886C>T
p.Arg296Trp

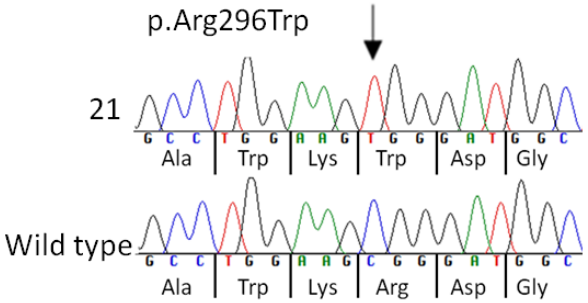

UCL-107

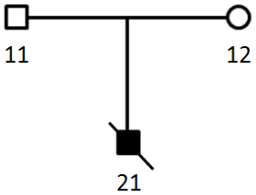

c.1232T>A
p.Ile411Asn

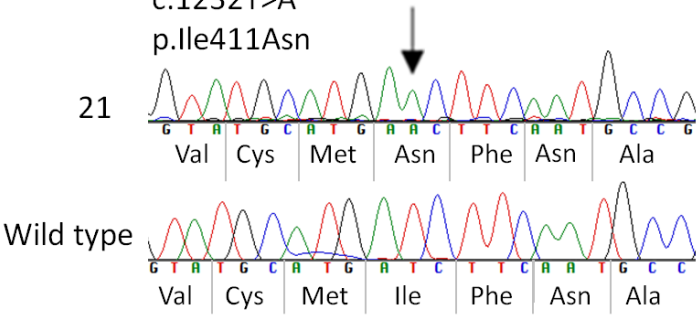

UCL-87

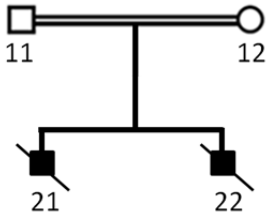

c.1232T>A
p.Ile411Asn

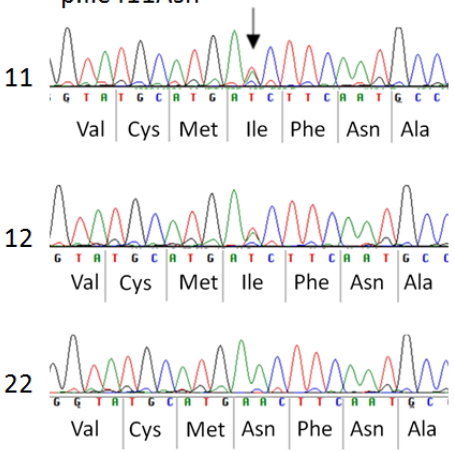

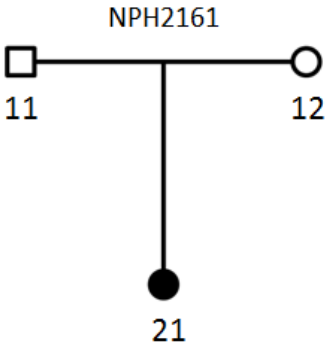

c.1390_1395del
p.[Asp464-Ile465del];[=]

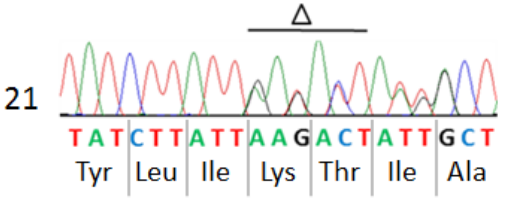

c.5179T>C
p.[Cys1727Arg];[=]

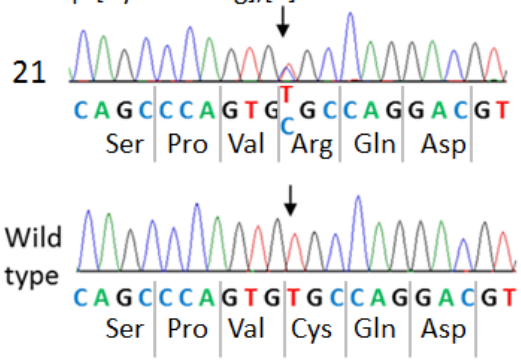

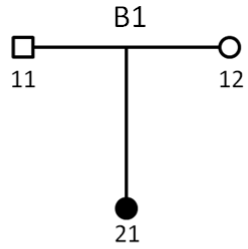

c.1671_1672dupAG
p.[Val558Glufs*12];[=]

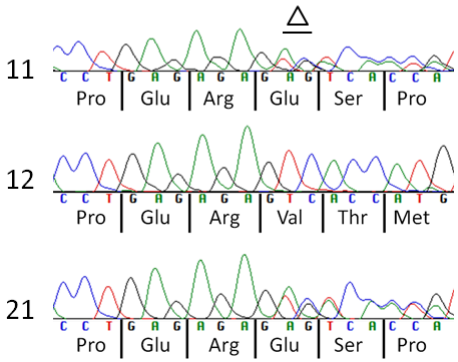

c.5179T>C
p.[Cys1727Arg];[=]

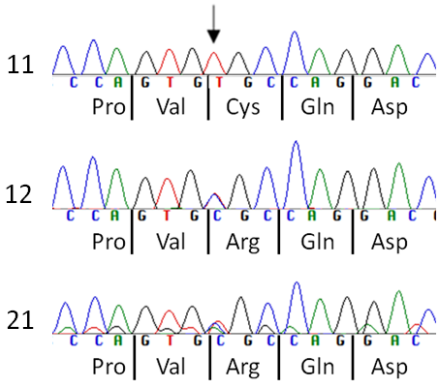

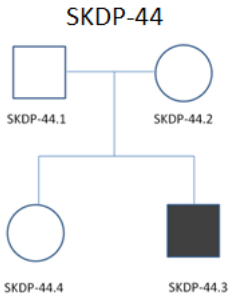

c.2158delC
p.[Arg720Valfs*28];[=]

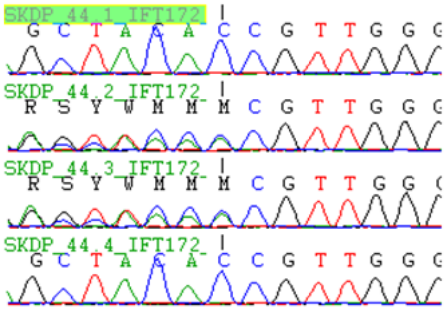

c.5179T>C
p.[Cys1727Arg];[=]

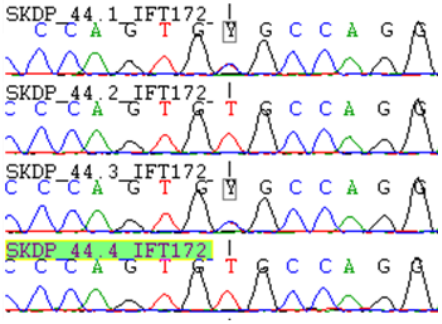

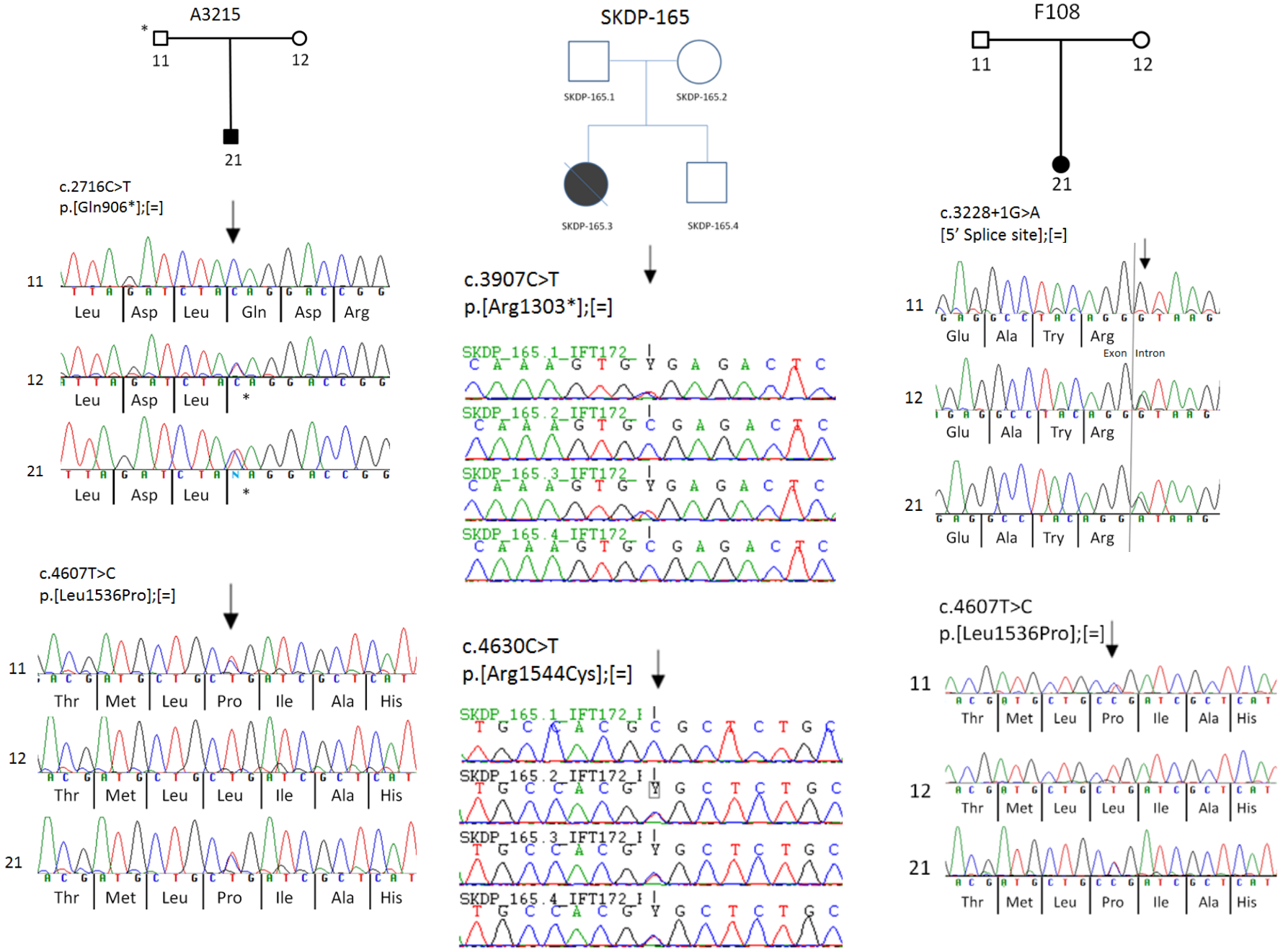
A3215
*
11
12
21
c.2716C>T
p.[Gln906*];[=]
11
Leu
Asp
Leu
Gln
Asp
Arg
12
Leu
Asp
Leu
*
21
Leu
Asp
Leu
*
c.4607T>C
p.[Leu1536Pro];[=]
11
Thr
Met
Leu
Pro
Ile
Ala
His
12
Thr
Met
Leu
Leu
Ile
Ala
His
21
Thr
Met
Leu
Pro
Ile
Ala
His
SKDP-165
SKDP-165.1
SKDP-165.2
SKDP-165.3
SKDP-165.4
c.3907C>T
p.[Arg1303*];[=]
SKDP_165.1_IFT172
SKDP_165.2_IFT172
SKDP_165.3_IFT172
SKDP_165.4_IFT172
c.4630C>T
p.[Arg1544Cys];[=]
SKDP_165.1_IFT172_I
SKDP_165.2_IFT172_I
SKDP_165.3_IFT172_I
SKDP_165.4_IFT172_I
F108
11
12
21
c.3228+1G>A
[5' Splice site];[=]
11
Glu
Ala
Try
Arg
Exon
Intron
12
Glu
Ala
Try
Arg
21
Glu
Ala
Try
Arg
c.4607T>C
p.[Leu1536Pro];[=]
11
Thr
Met
Leu
Pro
Ile
Ala
His
12
Thr
Met
Leu
Leu
Ile
Ala
His
21
Thr
Met
Leu
Pro
Ile
Ala
His

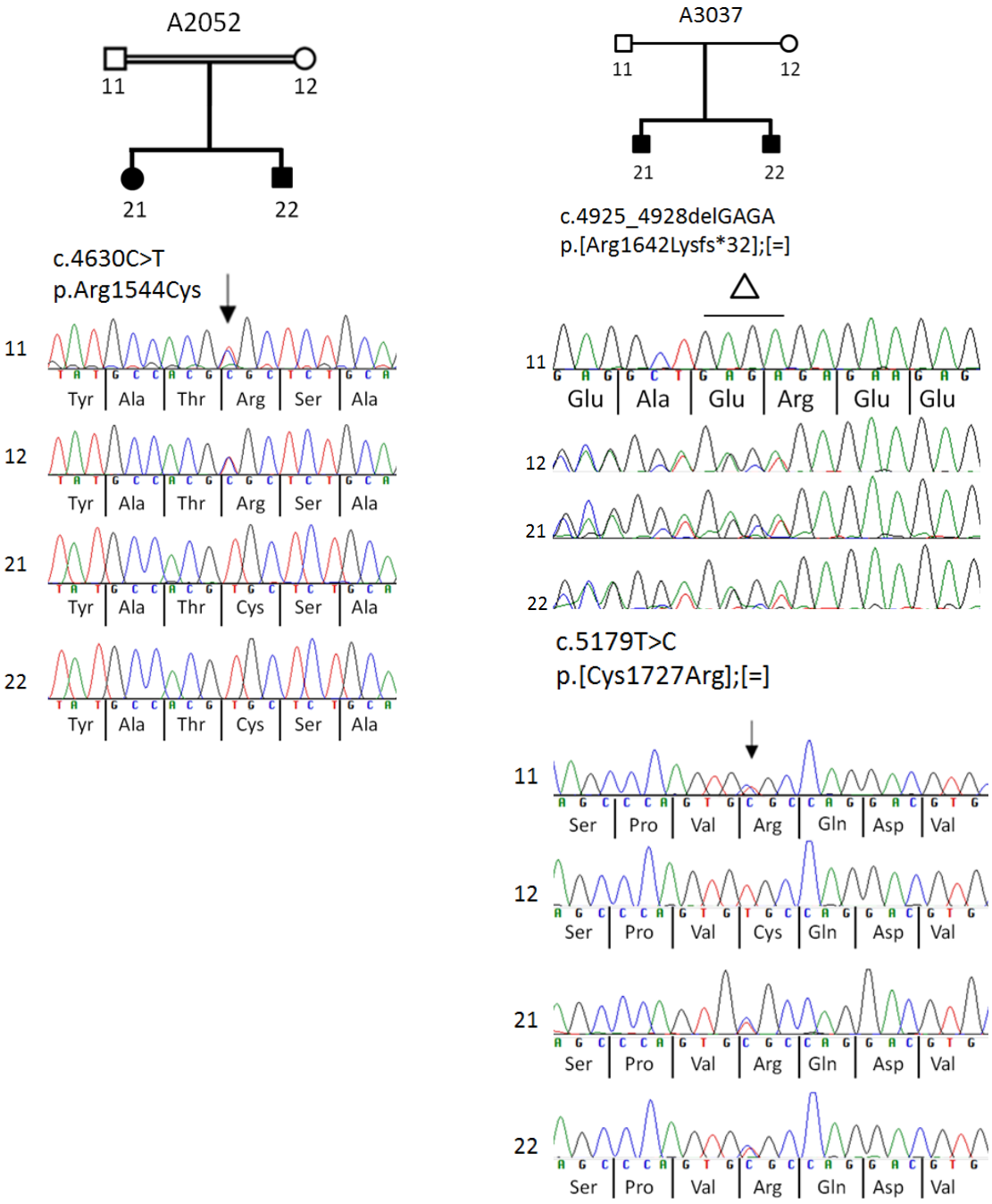

Figure S1. Recessive mutations in *IFT172* in 12 families with skeletal ciliopathies. Family numbers are shown above pedigrees. Mutation and predicted translational changes are indicated (see also **Table 1**). Sequencing traces are labelled according to the numbering in the family pedigree shown above. Where segregation was not available, sequence traces are shown for mutations above normal controls. Mutated nucleotide positions are indicated by arrows. Heterozygous mutations are bracketed, all others are homozygous.

[a]Mutation results in exon skipping (see **Figure S2**).

*Father has different phenotype (ADPKD) without skeletal abnormalities.

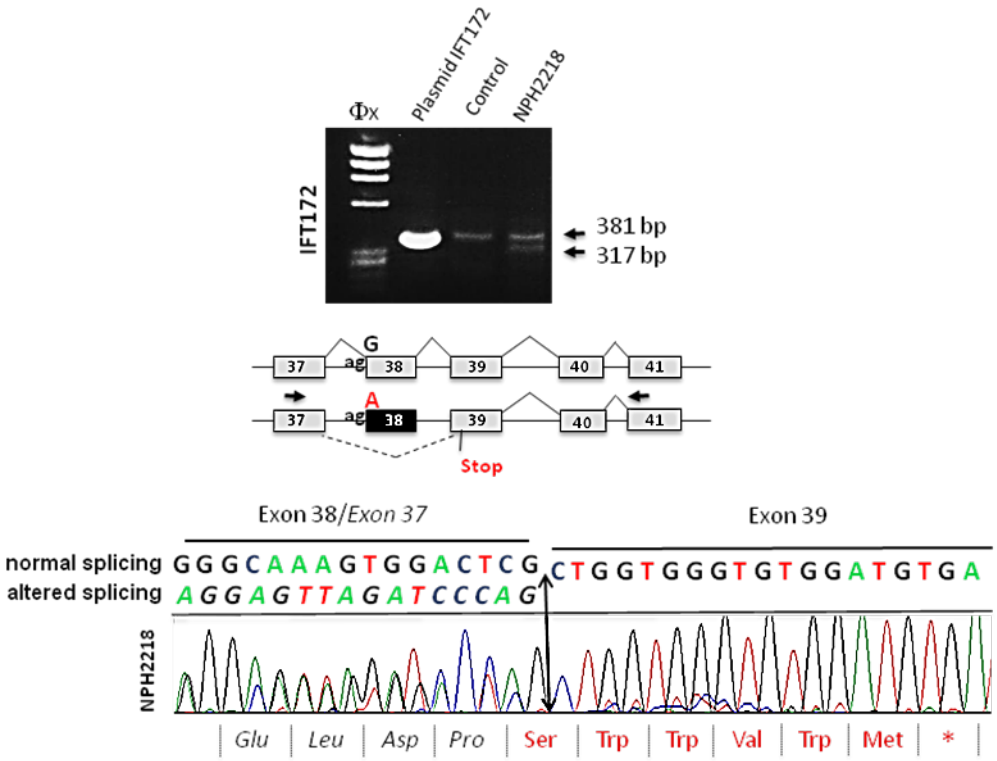

Figure S2. Pathogenicity of the 3' splice site mutation c.4161G>A in individual NPH2218. RT-PCR analysis of the *IFT172* transcript in patient NPH2218 fibroblasts harboring the c.4161G>A mutation in exon 38 and control individual using primers located in exons 37 and 41. In addition to the 381-bp band corresponding to normal splicing, a 317-bp band was detected from individual NPH2218 cDNA. Lane 1: Molecular weight marker Fx174 *Hae*III; lane 2: PCR product from human IFT172 plasmid; lane 3: RT-PCR product from control fibroblasts; lane 4: RT-PCR product from NPH2218 fibroblasts. Subsequent Sanger sequencing of the individual's (NPH2218) RT-PCR product revealed that the c.4161G>A mutation leads to aberrant splicing, with skipping of exon 38, resulting in a premature termination of the protein (p.Arg1387Serfs*7).

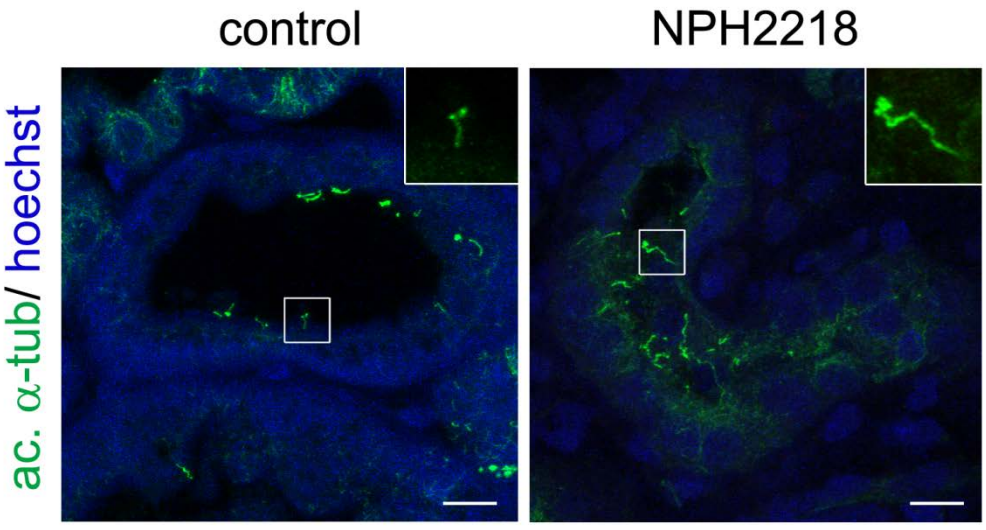

Figure S3. Cilia of kidney tubules of individual NPH2218. Paraffin-embedded kidney biopsy from control and individual NPH2218 were stained for acetylated alpha-tubulin. Cilia of the remaining tubules from individual NPH2218 appear not shortened, but even slightly elongated compared to control. Scale bar: 10µm.

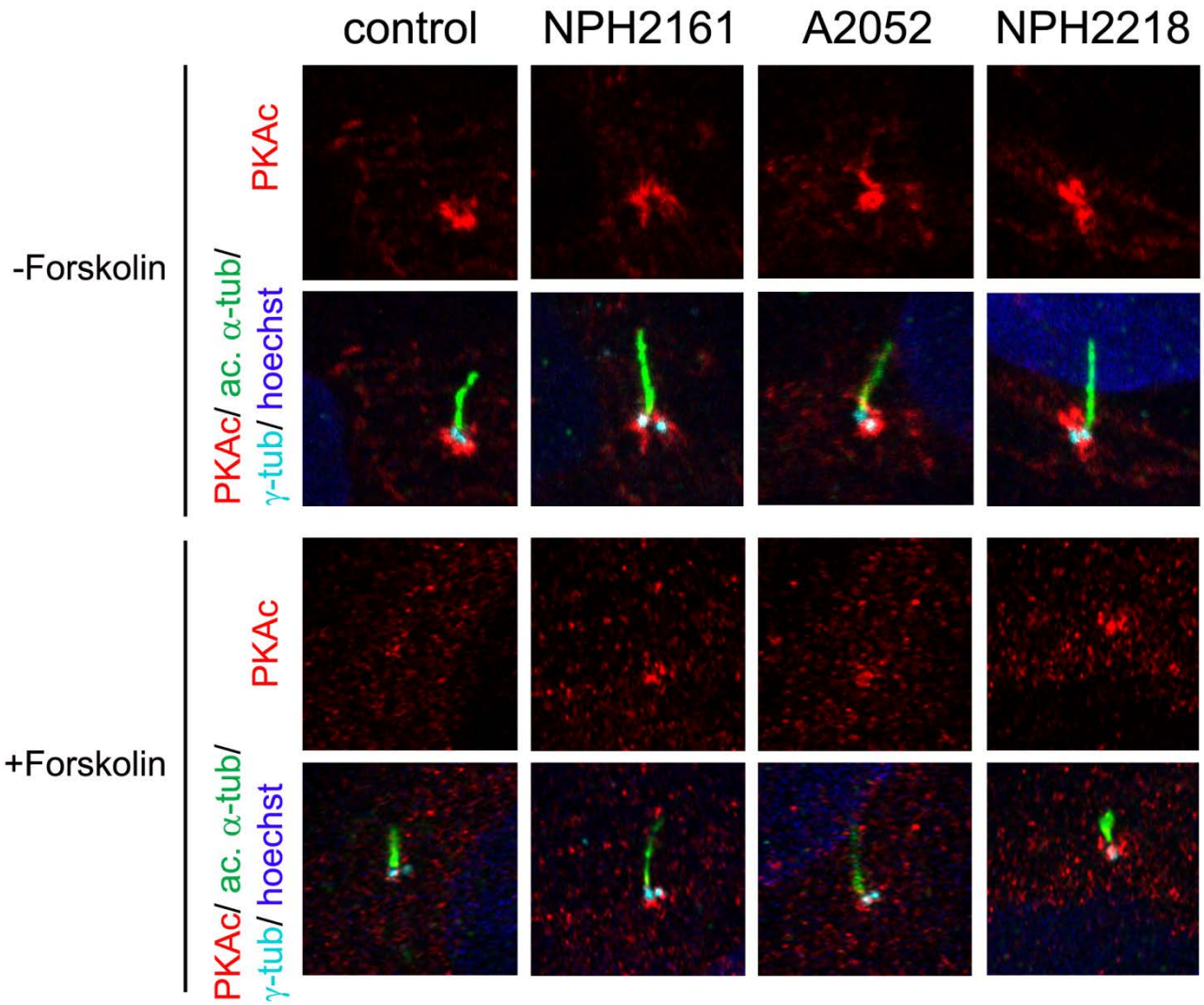

Figure S4. Abnormal PKAc redistribution in human fibroblasts from affected individuals after forskolin treatment. Control and mutant fibroblasts from individuals NPH2161, A2052 and NPH2218 were starved for 48hrs to induce ciliogenesis, treated with the adenylyl cyclase activator Forskolin for 1hr and then fixed with MetOH. Co-staining of PKA catalytic subunits (PKAc) using a mouse monoclonal antibody (BD Biosciences, 1:100), ARL13B and gamma-tubulin were perfomed and images were recorded with a SP8 confocal microscope and analyzed with ImageJ. As previously reported (Tuson *et al*. 2011), PKAc localizes at the base of the cilium in untreated cells. Following activation of adenylyl cyclase, PKAc is redistributed in the cytoplasm of control fibroblasts (as shown in Barzi *et al*. 2009) while an abnormal accumulation of PKAc remained at the base of the cilium in mutant fibroblasts, suggesting a defective PKA/adenylate cyclase signaling pathway.

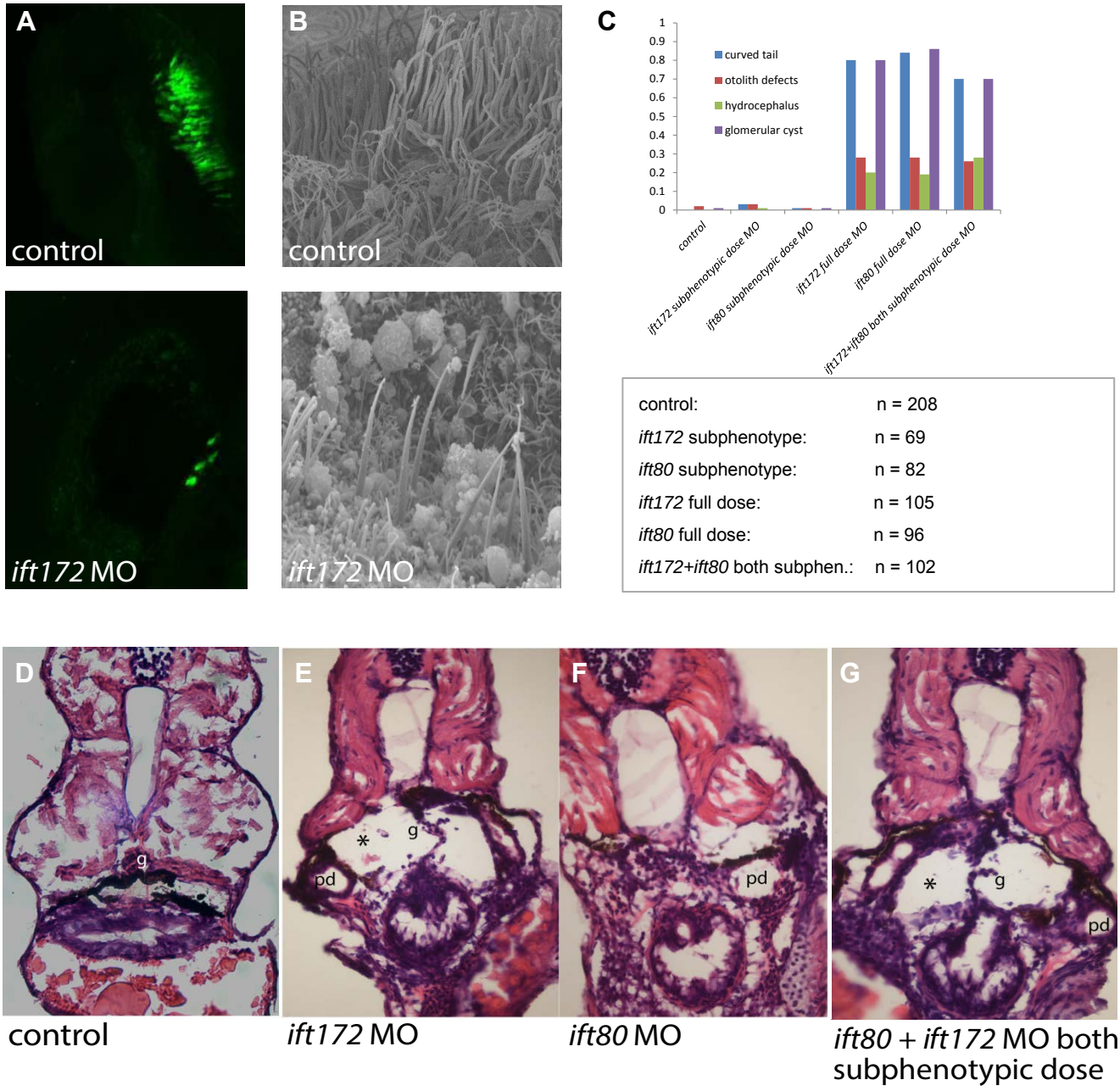

Figure S5. Knockdown of *ift172* in zebrafish. (A) Knockdown of *ift172* in a rhodopsin:GFP transgenic zebrafish line, shows retinal dystrophy at 4 dpf. **(B)** Scanning EM of olfactory pits in *ift172* morphants exhibits ciliogenesis defects. **(C)** Bar graph shows quantitative phenotypic findings after injection of each MO. **(D-G)** Zebrafish histology (zf-sections) of control **(D)**, *ift172* **(E)** and *ift80* **(F)** morphants as well as in morphants with the combined infection of subphenotypic doses of *ift172* and *ift80* **(G)**. Dilation of pronephric duct (pd) and occurrence of kidney cysts, as indicated by (*) in the two full dose morphants as well as in the morphant with the combined injection of *ift172* and *ift80*, when compared to control (g = glomerulus).

Table S1. 14 genes, encoding IFT-B components, included in mutation analysis in 1,056 individuals with NPHP-RC at University of Michigan.

No	*Gene symbol*	Gene name	Accession	Locus	# Exons
1	***IFT172/SLB***	intraflagellar transport 172 homolog (Chlamydomonas)	NM_015662.1	chr2:27,667,241-27,712,571	48
2	***IFT88***	intraflagellar transport 88 homolog (Chlamydomonas)	NM_175605.3	chr13:21,141,208-21,265,576	26
3	***IFT80***	intraflagellar transport 80 homolog (Chlamydomonas)	NM_020800.2	chr3:159,976,255-160,102,434	19
4	***IFT46***	intraflagellar transport 46 homolog (Chlamydomonas)	NM_020153.3	chr11:118,415,243-118,436,791	11
5	***IFT52***	intraflagellar transport 52 homolog (Chlamydomonas)	NM_016004.2	chr20:42,219,579-42,275,861	14
6	***IFT57/HIPPI***	intraflagellar transport 57 homolog (Chlamydomonas)	NM_018010.3	chr3:107,879,659-107,941,417	11
7	***IFT74/CCDC2***	intraflagellar transport 74 homolog (Chlamydomonas)	NM_001099222.1	chr9:26,956,371-27,062,931	19
8	***IFT81/CDV1***	intraflagellar transport 81 homolog (Chlamydomonas)	NM_001143779.1	chr12:110,562,140-110,656,600	18
9	***RABL5/IFT22***	RAB, member RAS oncogene family-like 5	NM_022777.2	chr7:100,956,648-100,965,093	5
10	***TRAF3IP1/IFT54***	TNF receptor-associated factor 3 interacting protein 1	NM_015650.3	chr2:239,229,185-239,309,541	17
11	***HSPB11/IFT25***	heat shock protein family B (small), member 11	NM_016126.2	chr1:54,387,234-54,411,288	4
12	***IFT20***	intraflagellar transport 20 homolog	NM_174887.2	chr17:26,655,353-26,662,495	5
13	***IFT27***	intraflagellar transport 27 homolog	NM_001177701.2	chr22:37,154,246-37,172,172	7
14	***TTC30B/IFT70***	tetratricopeptide repeat domain 30B	NM_152517.2	chr2:178,414,886-178,417,524	1

Table S2. Whole exome sequencing; final evaluation sheet of individual UCL-87.

FAMILY NAME	Gene	hg19	Accession #	Nt change c.	AA change p.	Zygosity	Conservation							Poly 2 (Hum Var)	Mut Taster	SIFT Score	1000-Genomes	EVS	Coverage	Biobase	Hom Peak
							Mm	Gg	Xt	Dr	Ci	Ce	Dm								
UCL 87	***IFT172***	chr2:27700177	NM_015662.1	c.1232T>A	p.Ile411Asn	Hom.	**I**	**I**	**I**	**I**	**I**	**I**	**I**	**0.89**	**DC**	**DC**	NA	NA	165	no	yes
	ERCC6	chr10:50679075	NM_000124.3	c.3016A>T	p.Thr1006Ser	Hom.	**T**	**T**	**-**	**T**	**T**	**R**	**-**	**0.69**	**DC**	**DC**	NA	NA	186	Yes[a]	yes
	PDE11A	chr2:178494176	NM_001077197.1	c.2011_2012insGGG	p.Ser671delinsTrpAla	Hom.	**D**	**E**	**Y**	**I**	**R**	**Q**	**-**	**ND**	**benign**	**ND**	rs67772336*	NA*	123	Yes[b]	no

a) ERCC6 (excision repair cross-complementing rodent repair deficiency, complementation group 6): gene is listed in Biobase as causing Cockayne Syndrome (#MIM133540), ref.24), this variant is not listed. b) PDE11A (phosphodiesterase 11A): gene is listed in Biobase as causing adrenocortical dysplasia and adenoma (PPNAD2, #MIM 610475, ref.23), this variant is not listed. *region is surrounded by known SNPs with three bp insertions.

be, Benign; Ce, Caenorhabditis elegans; Ci, Ciona intestinalis; DC, Disease-causing; Dm, Drosophila melanogaster; Dr, Danio rerio; Gg, Gallus gallus; Hom, homozygous; Hom Peak, variant is within a homozygous stretch; Mm, Mus musculus; NA, Not applicable; ND, No data; Xt, xenopus tropicalis.

References

1. Horvath, A., Boikos, S., Giatzakis, C., Robinson-White, A., Groussin, L., Griffin, K.J., Stein, E., Levine, E., Delimpasi, G., Hsiao, H.P., et al. (2006). A genome-wide scan identifies mutations in the gene encoding phosphodiesterase 11A4 (PDE11A) in individuals with adrenocortical hyperplasia. *Nat. Genet.* 38, 794-800.

2. Troelstra, C., van Gool, A., de Wit, J., Vermeulen, W., Bootsma, D., and Hoeijmakers, J.H.J. (1992). ERCC6, a member of a subfamily of putative helicases, is involved in Cockayne's syndrome and preferential repair of active genes. *Cell* 71, 939-953.

Table S3. Summary of identified variants for SKDP-165.3 and SKDP-44.3

	SKDP-165.3	**SKDP-44.3**
Number of variants identified (minor allele freq 0.05 or lower)	39866	61520
Number of variants after QC, including coverage filters and correction for platform and alignment artefacts	1985	1819
Nonsynonymous SNPs or indels in exons or splice sites after QC	1023	1061
Rare (MAF <0.001) variants after filtering as above	262	283
≥2 variants per gene, after filtering as above	37	18
Remaining variants filtered as above, not predicted to be benign by Polyphen	29 (7 genes ≥ 2 hits *IFT172, STXBP5L, CLDN1, TRIM5, DNAH3, FHOD3, DRG1*)	17 (4 Gene ≥ 2 hits *IFT172, DNAH6, MYO7B, SMG1*)
Number of genes with rare (MAF<0.001) nonsynonymous SNPs and indels in exons or splice sites after QC with ≥2 variants predicted to be damaging by Polyphen, reported in Ciliome[1]	4 (*IFT172, STXBP5L, DNAH3, DRG1*)	3 (*IFT172, DNAH6, SMG1*)
Number of genes as above, with appropriate segregation of variants within the family	2 *(IFT172, STXBP5L)*	1 (*IFT172*)

*MAF – minor allele frequency; QC – quality control

Reference

1. Inglis, P.N., Boroevich, K.A., and Leroux, M.R. (2006). Piecing together a ciliome. Trends in genetics : TIG 22, 491-500.

Table S4. Summary statistics for mapping and coverage for SKDP-165.3 and SKDP-44.3.

	SKDP-165.3	SKDP-44.3
Total bases	3902939063	5165816727
Bases on target exons (+/-200bp)	3178163279	4086677612
Bases on target exons	2274600176	2771959624
% bases on target exons (+/- 200bp)	81	79
% bases on target exons	58	54
Target exon median base coverage	35	40
Target exon mean base coverage	40	44
% target exon bases with coverage >1	94	94
% target exon bases with coverage >5	89	92
% target exon bases with coverage >10	83	88
% target exon bases with coverage >15	75	83